Optimal Coverage Path Planning for Arable Farming on 2D Surfaces

J. Jin, L. Tang

Abstract. *With the rapid adoption of automatic guidance systems in agriculture, automated path planning has great potential to further optimize field operations. Field operations should be done in a manner that minimizes time and travel over field surfaces and should be coordinated with specific field operation requirements, machine characteristics, and topographical features of arable lands. To reach this goal, an intelligent coverage path planning algorithm is the key. To determine the full coverage pattern of a given field by using boustrophedon paths, it is necessary to know whether to and how to decompose a field into sub-regions and how to determine the travel direction within each sub-region. A geometric model was developed to represent this coverage path planning problem, and a path planning algorithm was developed based on this geometric model. The search mechanism of the algorithm was guided by a customized cost function resulting from the analysis of different headland turning types and implemented with a divide-and-conquer strategy. The complexity of the algorithm was analyzed, and methods for reducing the computational time are discussed. Field examples with complexity ranging from a simple convex shape to an irregular polygonal shape that has multiple obstacles within its interior were tested with this algorithm. The results were compared with other reported approaches or farmers' recorded patterns. These results indicate that the proposed algorithm was effective in producing optimal field decomposition and coverage path direction in each sub-region.*

Keywords. *Auto guidance, Boustrophedon path, Coverage path, Field decomposition, Optimal path planning, Turning cost.*

With the rapid adoption of automatic guidance systems in agriculture, automated path planning has potential to further optimize field operations. In the meantime, with the trend toward larger farms and corporate farming, the use of low-skilled or contracted labor is ever increasing, making automatic path planning practically valuable. Field operations should be done in a manner that minimizes time, minimizes travel over field surfaces, and is coordinated with specific field operation requirements, machine characteristics, and topographical features of arable lands. In this way, the efficiency of different field operations can be maximized. Current applications of automatically guided field equipment only enable the machine to follow parallel straight or contour paths that provide complete field coverage, and little operational optimization has been taken into account, especially when irregular field boundaries are present. To improve field efficiency and, in particular, to fully utilize the advantages provided by automatically guided farming equipment, an optimal coverage path planner is of great importance.

Some coverage path planning research has been reported, but there has been no complete solution in the context of arable farming. Fabret et al. (2001) approached the coverage path planning problem by formulating it as a "traveling salesman problem" (TSP). In their approach, a "steering edge" of the field was chosen that provided a direction in which to guide the successive swaths. Then a series of "characteristic points" in the headland of the field was collected, and an "associated graph" was constructed using a TSP solver to connect those points by the lines in the steering direction. However, this work did not report the strategy of how the "steering edge" was chosen. Ryerson and Zhang (2007) used grid representation for the field, and a genetic algorithm was used to find the optimal path traveling though all the grids (thus covering the whole field). However, the research did not provide paths that covered the field completely. In addition, the algorithm was only tested on a simple-shaped field (with a rectangular boundary and one rectangular obstacle inside). As the field shape becomes complex (as in real cases), the developed algorithm might not be feasible. Yang and Luo (2004) applied neural networks for coverage path planning. The simulation results from their work showed that the proposed model was capable of planning collision-free complete coverage robot paths. However, the collision-free requirement is not a priority in coverage planning for arable farming. Coverage costs, such as the cost of turnings at the edges, were not investigated by this model, thus making it not necessarily optimal for farm field coverage planning.

When designing an optimal coverage path planner that can cope with field boundary irregularities, field decomposition has a potential to further improve the field efficiency of farming equipment before determining the best path direction of a given field. If the whole field can be decomposed into several sub-regions, which can reduce the overall cost in terms of time required for field equipment to fully cover the entire operational surface, then a proper field decomposition

Submitted for review in July 2009 as manuscript number IET 8099; approved for publication by the Information & Electrical Technologies Division of ASABE in February 2010. Presented at the 2009 ASABE Annual Meeting as Paper No. 097274.

The authors are **Jian Jin,** Graduate Student, and **Lie Tang, ASABE Member Engineer,** Assistant Professor, Department of Agricultural and Biosystems Engineering, Iowa State University, Ames, Iowa. **Corresponding author:** Lie Tang, Department of Agricultural and Biosystems Engineering, Iowa State University, 203 Davidson Hall, Ames, IA 50010; phone: 515-294-9778; fax: 515-294-6633; e-mail: lietang@iastate.edu.

  ISSN 2151-0032

process has to take place simultaneously with the path direction searching process. So far, the only field decomposition method adopted in coverage path planning is the trapezoidal decomposition method. Trapezoidal decomposition is a popular method for subdividing a field (Berg et al., 2000). In the decomposition process, a direction is chosen, and a set of parallel lines is drawn in this direction through all the vertices of the field boundary. The field is then divided by these lines into a trapezoidal map. Choset and Pignon (1997) and Oksanen and Visala (2007) adopted the trapezoidal decomposition method for coverage path planning. However, their work did not include detailed discussions of how to determine the direction of the trapezoidal decomposition lines, and there was little evidence that these parallel lines could provide the best decomposition of a given field with regard to minimizing the coverage costs.

The most important component in coverage path planning is to determine the best direction of the paths. For agricultural field operations, boustrophedon paths (straight parallel paths with alternate directions) represent the most straightforward approach since they can be easily followed by agricultural equipment. Given a field, once an optimal coverage direction is determined, the whole field can usually be covered by boustrophedon paths guided by this direction. There are several methods for finding the optimal path direction. The simplest way is to follow the longest edge of the field (Fabret et al., 2001), but following the longest edge is only suitable for fields with a simple convex shape, such as rectangular. To achieve a generic solution for coverage path planning, irregularities of field boundaries have to be considered. One such attempt was first made by Oksanen and Visala (2007), who used a search algorithm to find an optimal trapezoidal splitting direction (same as the path direction) between 0° and 180° according to an unspecified cost function. In each round of the algorithm, the field was first split into trapezoids based on the chosen direction, and the trapezoids were merged into larger blocks. Then the largest or most efficient driving block of the field was selected using certain criteria, including the area and the route length of the block and driving efficiency. Once the trapezoidal block was selected, it was covered along the splitting direction and removed from the original field. The same algorithm was then applied iteratively for the rest of the field until the paths of the whole field path were computed. However, an optimized decomposition could not be guaranteed in their approach, leading to a splitting direction that was not necessarily the most efficient path direction. For the purpose of searching for an optimal coverage path planning solution, a decomposition and direction search algorithm for minimizing headland turning cost based on an accurate computational model is desired.

The overall objective of this research was to better understand how a 2D optimal coverage path planner could minimize the operational time required for agricultural field equipment to cover a field. This research had the following specific objectives:

- To formulate the coverage path planning problem as an optimization problem and to investigate a search algorithm for finding the optimal field decomposition and path directions for the coverage of planar fields.
- To evaluate the effectiveness of the developed optimal coverage path planner.

METHODS

The algorithm developed for optimal coverage path planning for arable farming on 2D surfaces contained several steps. First, a geometric representation of the field shape was adopted for the formulation of the 2D path planning problem. Second, the optimal path direction and the optimal field decomposition were searched to solve the problem. To search for the optimal path direction, the cost function of the angled turns was defined. Multiple headland turning types might be available, and the turning cost depended on the adopted headland turning type at each field edge. The costs of several of the most commonly used headland turning types were analyzed, and the method for selecting the most suitable turning type was developed. To search for the optimal decomposition, a topological undirected graph was built for finding all possible dividing lines. The details of these steps are described below, and the general algorithm is summarized at the end of this section.

PROBLEM FORMULATION

To develop an optimal coverage path planner, a geometric model for defining the inputs and outputs of the planning algorithm must be developed. A field has only one outside boundary, which commonly contains straight edges. If the field boundary contains curves, then the curves can always be approximated by chains of line segments connecting sampled points on the curves. The more points are sampled, the more accurately the curve is approximated. Therefore, the outside contour of a field can always be represented as a polygon. There may also be non-passable obstacles within the field, such as ponds, trees, and some waterways. Similarly, these obstacles can be represented by polygonal holes within the polygonal outside boundary of the field. As a result, a farm field can be represented as one outside boundary polygon and a number of smaller inside polygons that represent obstacles (fig. 1). For a 2D field, this is a planar subdivision that can be represented by a data structure called “doubly connected edge list” (DCEL) (Muller and Preparata, 1978).

For farm field coverage path planning, it is critical to find the best way to decompose a field into multiple sub-regions and the corresponding best path direction for each region, such that the total cost of covering these regions with boustrophedon paths can be minimized. To summarize, the input of a farm field coverage path planning problem is a planar subdivision representing the field as well as some other parameters, such as the operation width, the vehicle’s minimum

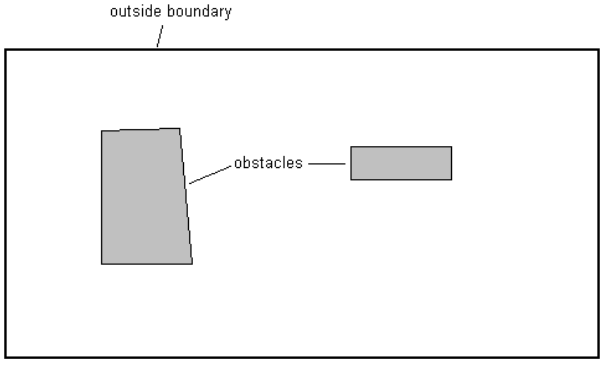

Figure 1. Farm field with non-passable obstacles within the field could be represented as a planar subdivision.

turning radius, and headland width, while the output is a list of planar subdivisions, with each representing a divided subregion that is also marked with the best path direction.

General Description of the Turning Cost Function

For coverage path planning, coverage efficiency is of the highest concern. Coverage efficiency is inversely related to total operational time. While operating along straight sections of the boustrophedon paths in the interior of a field, with 2D coverage path planning, the speed and the total travel distance (which can be calculated as the field area divided by the swath width) are almost constant. Therefore, the cost on the straight path sections in the interior of the field is almost constant, and the total coverage cost is primarily determined by the cost of the headland turning parts of the paths.

In order to reduce the total turning cost, the number of turns needs to be minimized. In addition, turns with relatively high operational costs need to be avoided. Fields of irregular shapes have inefficiencies related to headland turns when headlands are at an angle to machine travel (Hunt, 2001). For an angled turn, as shown in figure 2, the total travel distance in the headland is dramatically increased compared with the case when the headland is orthogonal to the machine travel. This extra travel distance causes losses in time and operator effort.

The number of turns on the ith edge (N_i) depends on the length of the edge and the angle between the edge and the machine travel direction. N_i is calculated as:

$$N_i = L_i \left| \sin(\theta - \varphi_i) \right| / 2w \tag{1}$$

where L_i is the length of the edge, w is the swath width, θ is the swath direction, and φ_i is the edge direction.

Assuming that the turning cost in figure 2 can be estimated as C_{turn}, except for the situation where the path and the edge are parallel or nearly parallel, the cost on the ith edge is:

$$C_i = C_{turn} \cdot N_i \tag{2}$$

The total turning cost of covering a field with boustrophedon paths along direction θ is thus the sum of costs on all edges, including the edges of the internal obstacles in the field. The total cost is then computed as:

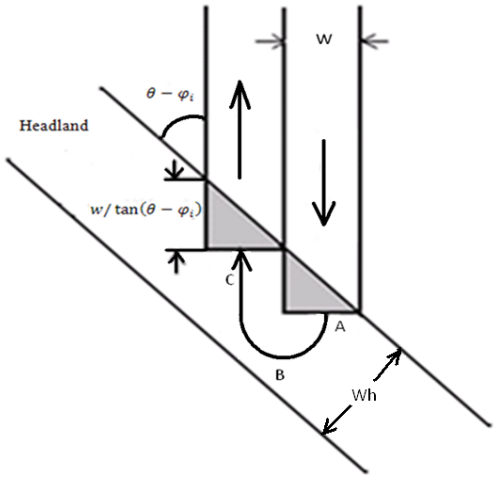

Figure 2. Illustration of an angled turn: w is the swath width, θ is the swath direction, and φ_i is the edge direction.

$$C = \sum_{i=1}^{p} C_i \tag{3}$$

where p is the number of field edges.

The objective of optimization is to minimize C by choosing a value of θ for $\theta \in [0,180°)$. The following subsection provides detailed analysis of the turning cost (C_{turn}) for different headland turning types.

Cost Analysis of Different Headland Turning Types

As described above, the criterion was to have an accurate estimation of C_{turn}. In figure 2, it is assumed that a "U" turn (the trajectory A-B-C) could be made. However, due to the restricted minimum turning radius of the field equipment, predefined row width, and limited headland space, a "U" turn might not be applicable in some situations. In addition, even when a "U" turn is applicable, it is not always the most cost-effective turn. Instead, another headland turning type, such as "flat" turn, "bulb" (keyhole) turn, "hook" (asymmetric bulb) turn, or "fishtail" turn, is more efficient. In the following sections, different headland turning types are investigated and compared.

Case 1: "Flat" Turn

When the vehicle and implement turning radius is smaller than half the swath width ($r < w/2$), a "flat" turn can be made instead of a conventional "U" turn with a larger turning radius (the dashed curve in fig. 3). When the center point of the implement reaches point A, part of the implement starts to exit the interior of the field. However, in order to completely finish the coverage of the current swath, the vehicle needs to keep moving straight ahead until point B is reached. The vehicle then makes the "flat" turn from B to C and starts to reenter the field from D, until the entire width of the implement is inside the field from point E. This headland turning type will save headland space and reduce the length of the total turning trajectory, and thus reduce the time cost of turning.

Assuming v is the turning speed, the time cost on this turn (from B to D) is:

$$C_{turn} = \frac{w(1+\cot\theta) + r(\pi - 2)}{v} \tag{4}$$

This same turning speed v is also assumed for other headland turning cases.

Case 2: "U" Turn

A "U" turn happens at the critical state of the "flat" turn when $r = w/2$ (fig. 4). Similarly, the time cost of a "U" turn is:

$$C_{turn} = \frac{(\pi + 2\cot\theta)w}{2v} \tag{5}$$

Case 3: "Bulb" Turn

When $r > w/2$, there is not enough space for the vehicle to make a "flat" turn or "U" turn, and a "bulb" turn is needed. To make a "bulb" turn, the vehicle starts by turning to the opposite direction first to make enough turning space (E-F), then turns back (F-G), and finally reverses the turning direction again (G-H) to enter the next swath (fig. 5).

In the case of a "bulb" turn, as shown in figure 5, the vehicle starts from the field exit at point E, when the vehicle is still traveling in alignment with the swath direction. The curve ends when the vehicle re-enters the field at point H,

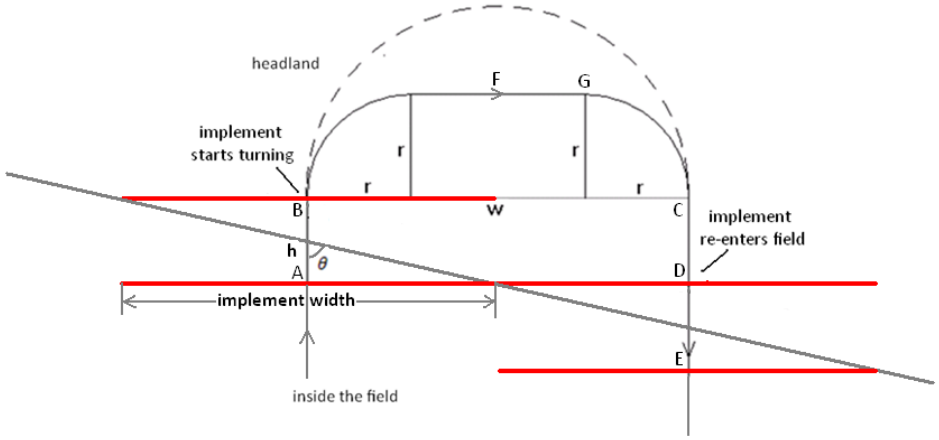

Figure 3. "Flat" turn made in headland when $r < w/2$. The dashed curve is a "U" turn to be compared.

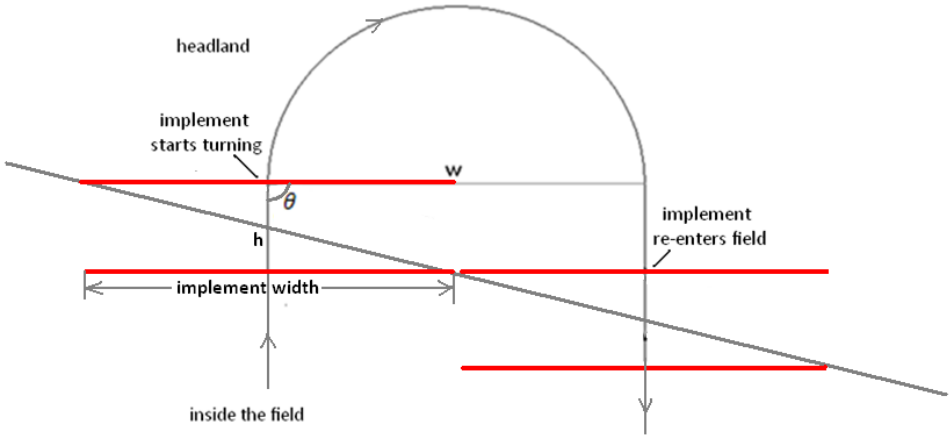

Figure 4. "U" turn made in headland when $r = w/2$.

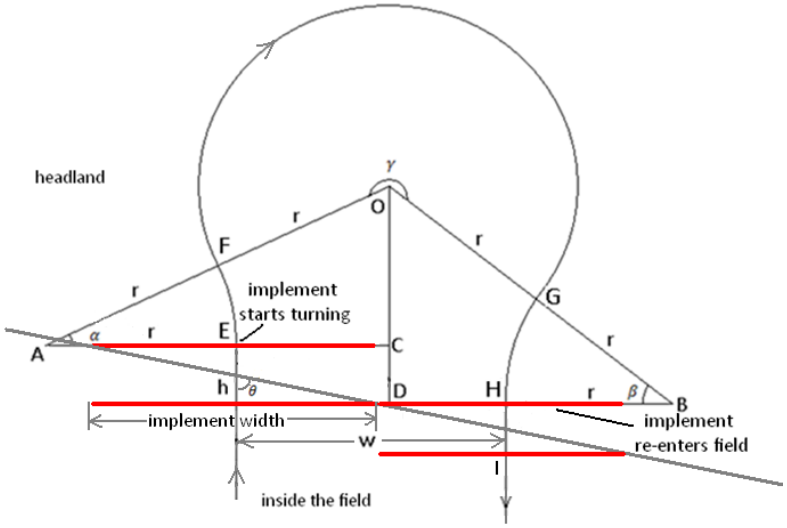

Figure 5. "Bulb" turn made in headland when $r > w/2$.

where the vehicle must be heading along the direction of the swath again. Theoretically, to ultimately save headland space and reduce the turning distance, the vehicle should always be turning with its minimum turning radius (r).

The headland width also imposes a limitation on "bulb" turns. The headland provides enough space for a "bulb" turn only if:

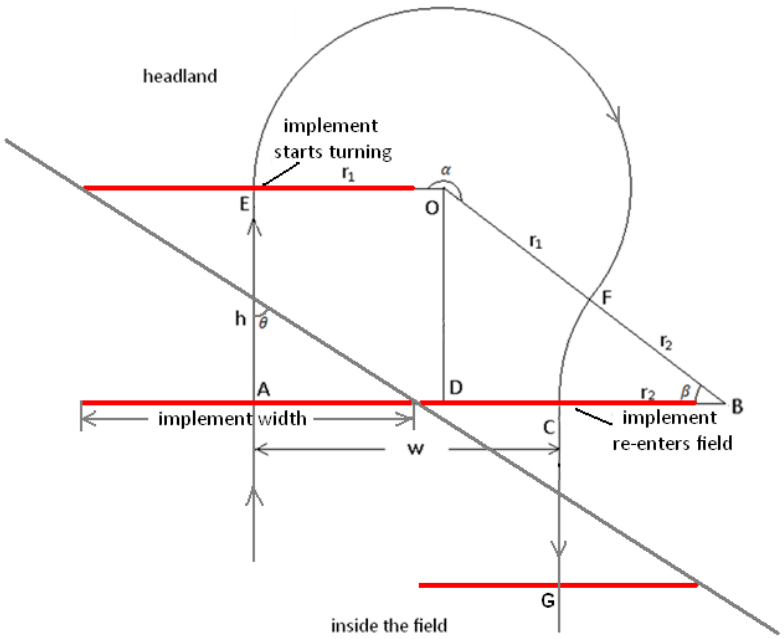

Figure 6. "Hook" turn made in headland when $r > w/2$.

$$W_h > r[1 + 2\sin\theta\sin\alpha + 2\cos\theta\cos\alpha - \cos\theta + (w/2)] \quad (6)$$

where W_h is the headland width, r is the vehicle's minimum turning radius, α is the angle of section EF in figure 5, θ is the angle between swath direction and the edge, and w is the operation width.

From geometric analysis of figure 5, the following equations were derived:

$$h = w/\tan\theta \quad (7)$$

$$\alpha + \beta = a\cos\left(\frac{w}{2r} + \frac{h^2 + w^2}{8r^2} - \frac{1}{2}\right) \quad (8)$$

where h and β are as indicated in figure 5. Hence, the time cost of this "bulb" turn was:

$$C_{turn} = r(\alpha + \beta + \gamma)/v \quad (9)$$

Since $\gamma = \pi + \alpha + \beta$, from equations 7, 8, and 9, the cost function of the bulb turn was obtained as:

$$C_{turn} = r\left[\pi + 2a\cos\left(\frac{w}{2r} + \frac{w^2(\tan^2\theta)}{8r^2\tan^2\theta} - \frac{1}{2}\right)\right]/v \quad (10)$$

Case 4: "Hook" Turn (Asymmetric "Bulb" Turn)

When $r > w/2$, another headland turning type, called a "hook" turn, can be applied instead of a "bulb" turn. Rather than starting by turning toward the opposite direction, as the "bulb" turn does, a "hook" turn starts like a "U" turn. When reaching point F, it reverses the turning direction and adjusts to the next adjacent swath (fig. 6).

The turning trajectory of a "hook" turn in the headland consists of two sections: EF and FC (fig. 6). Again, as in the case of a "bulb" turn, theoretically the vehicle should be turning with its minimum turning radius for section EF to maximally save headland space and reduce the turning distance. For section FC, the turning radius needs to be chosen so that the vehicle will fit the next adjacent row when reaching point C, resulting in the following equations:

$$r_1 = r \quad (11)$$

where r is the minimum turning radius of the vehicle, and:

$$r_2 > r_1 \quad (12)$$

From geometric analysis of figure 6, we can further derive the following:

$$r_2 = \frac{w^2\cot^2\theta + w^2 - 2wr}{4r - 2w} \quad (13)$$

$$\beta = \sin^{-1}\frac{4rw\cot\theta - 2w^2\cot\theta}{4r^2 - 4wr + w^2\cot^2\theta + w^2} \quad (14)$$

Combining equations 12 and 13, the "hook" turn can be a feasible solution only when:

$$4r^2 \le h^2 + w^2 \quad (15)$$

or equivalently:

$$r \le \frac{w}{2\sin\theta} \quad (16)$$

In figure 6, equation 16 actually means that EC needs to be longer than $2r$ for a "hook" turn to be feasible. This situation tends to happen when θ is larger. In addition, as in the case of a "bulb" turn, a "hook" turn can also face the problem of limited headland width. A "hook" turn requires less turning space than a "bulb" turn, and the headland provides enough space for a "hook" turn only when:

$$W_h > r(1 + \cos\theta) + \frac{w}{2} \quad (17)$$

The time cost of this turn is:

$$C_{turn} = (r_1 \alpha + r_2 \beta) / v \quad (18)$$

Since $\alpha = \beta + \pi$, from equations 13, 14, and 18, the cost function of the "hook" turn is:

$$C_{turn} = \left(r\pi + \frac{4r^2 - 4wr + w^2 \cot^2\theta + w^2}{4r - 2w} \times \sin^{-1} \frac{4rw\cot\theta - 2w^2 \cot\theta}{4r^2 - 4wr + w^2 \cot^2\theta + w^2} \right) / v \quad (19)$$

Case 5: Headland Turning Types with Limited Headland Width

When headland width is smaller than the critical case shown in figure 7, none of the above headland turning types can be applied. The critical situation is expected when:

$$W_h = r(1+\cos\theta) + \frac{w}{2}(1+\sin\theta\cos\theta) \quad (20)$$

When $W_h < r(1+\cos\theta) + \frac{w}{2}$, the headland space is too limited for the normal headland turning types, and other types incorporating reversing are needed. For example, a "fishtail" turn (or switchback turn) has been used in practice. Kise et al. (2002) created switchback turning paths by applying a third-order spline function based on constraints including minimum turning radius and maximum steering speed. However, different-angled turns were not considered, and the discussion was based on the assumption that the path direction was orthogonal to the field edge. In addition, other constraints, such as limited headland width, were not included. The turning cost of those reversed types of turns depends largely on the vehicle's motion characteristics, which can hardly be described with a universal cost function as in the cases of other turning types. Analysis of "fishtail" turning costs remains as future work. Nevertheless, it can be expected that the cost of reversed turns in limited headland space would be higher than that of other headland turning types when $W_h \geq r(1+\cos\theta) + \frac{w}{2}(1+\sin\theta\cos\theta)$.

Selection of Headland Turning Types

When $W_h > r(1+2\sin\theta\sin\alpha+2\cos\theta\cos\alpha-\cos\theta) + \frac{w}{2}$ (eq. 6) and $r \leq \frac{w}{2\sin\theta}$ (eq. 16), both "bulb" turn and "hook" turn are applicable. The operational costs of these two types of turns need to be compared to make the choice. The ratio of turning cost of a "bulb" turn to a "hook" turn was calculated as a function of r, w, and θ (fig. 8). The upper-right flat "zero" area in figure 8 is an invalid area since $r > \frac{w}{2\sin\theta}$ for those points. For valid points, the ratios were always less than 1, which means "bulb" turns always have shorter turning distances than "hook" turns. However, "hook" turns have their advantages, too. First, "hook" turns require less headland width. It can be verified mathematically that equation 6 is a more restricted condition than equation 17. Second, since the turning radius of the FC section in figure 6 is larger, it is easier for the vehicle to adjust to the next adjacent swath before entering the field again. So the choice between a "bulb" turn and a "hook" turn could still depend on farmers' preference.

Similar to the choice between "bulb" turn and "hook" turn, the choice among all the five headland turning types described above depends on the swath width, headland width, minimum turning radius, and the angle between swath and edge. The restrictions and conditions for each headland turning type are summarized in a decision tree in figure 9.

Finding Dividing Lines

Since the goal of this optimal path planning application was to output a list of planar subdivisions that are also marked with the best path directions, all subdividing schemes needed to be found and evaluated. In this case, a topological undirected graphwas constructed as the tool for the searching task. The undirected graph was first generated from the planar subdivision representation of the field, which was the input of the algorithm. New points and edges were then added to the graph: all the diagonals were added, and from each vertex (including the vertices on the internal holes), rays were drawn into the internal area of the field (fig. 10a). Each ray

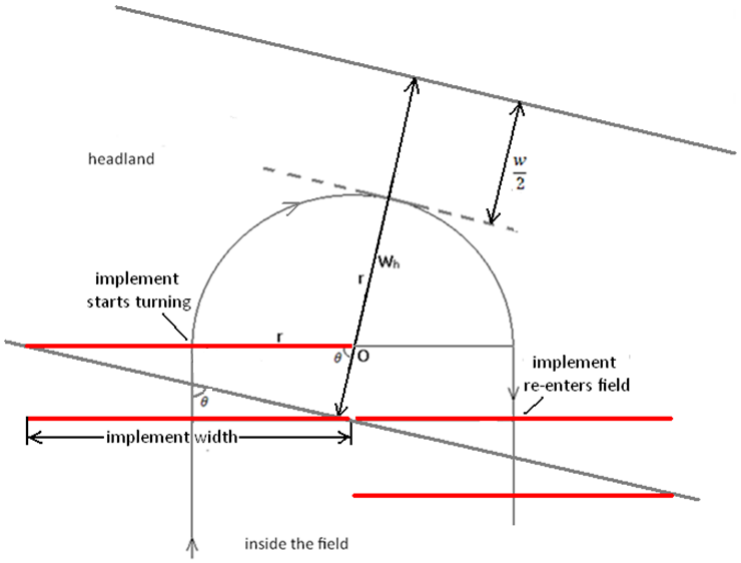

Figure 7. Minimum headland width for all turning types in cases 1 through 4.

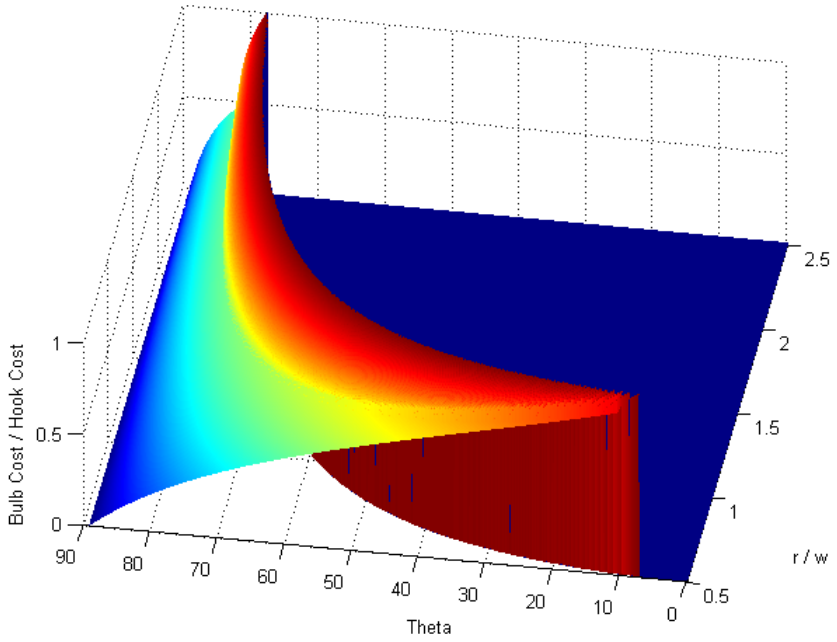

Figure 8. Ratio of turning cost of a "bulb" turn to a "hook" turn as a function of swath width (*w*), minimum turning radius (*r*), and angle between swath and edge (theta). The upper-right flat "zero" area is an invalid area where neither of the two headland turning types is feasible.

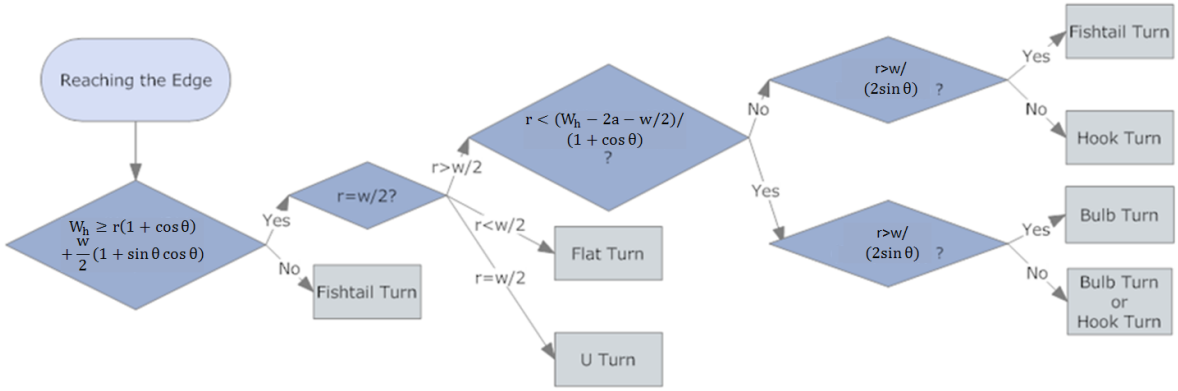

Figure 9. Decision tree for determining the most feasible headland turning type, where *r* is the minimum turning radius of the vehicle, θ is the angle between the swath and headland boundary, *w* is the swath width, *Wh* is the headland width, and α is the angle of arch EF in figure 5, which is a function of *r*, θ, and *w*.

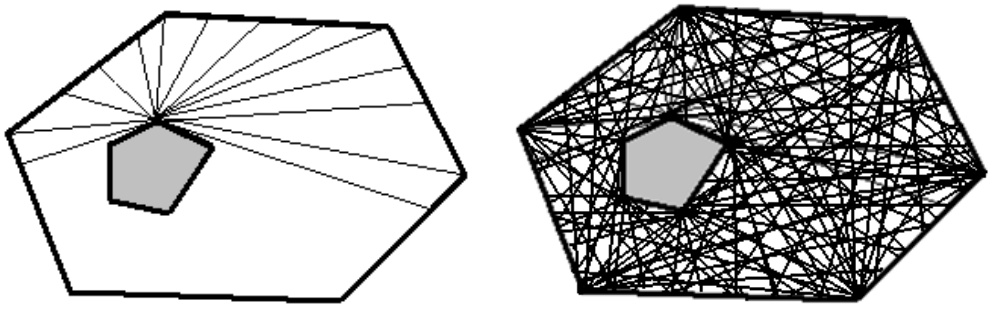

(a) **(b)**

Figure 10. Building the undirected searching graph: (a) drawing rays from a vertex, and (b) constructed undirected graph. (The actual step size for drawing the rays should be much smaller to find the optimal decomposition scheme).

must intersect with an edge of the original polygons. The step size for drawing the rays (the angle between two neighboring rays) determined how precisely the optimal decomposition scheme could be constructed. Once all the rays from all vertices were drawn, the new undirected graph was built subsequently (fig. 10b), where the vertices in the planar subdivision and the new intersection points corresponded to the vertices in the graph, while the edges in the planar subdi-

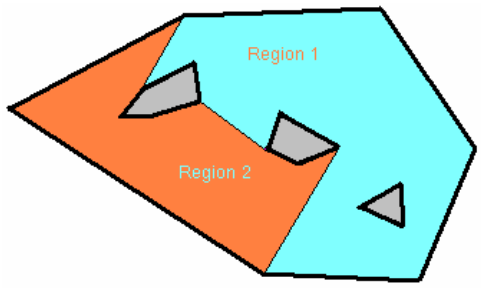

Figure 11. Example of a dividing line between two regions.

vision and the newly drawn line segments corresponded to the edges in the graph.

Once the graph was constructed, depth-first searches were conducted in the graph to find all possible lines that divided the whole field into two sub-regions. Each search resulted in a dividing line composed of a sequence of edges in the graph, which divided the whole field into two sub-regions. Specifically, each search started from a vertex on the outside boundary. Whenever the search reached another vertex on the outside boundary or itself, a new dividing line was formed, which was actually a chain of edges in the graph. Figure 11 shows such a dividing line. It could be proved that all such dividing lines would be found by the depth-first search.

General Algorithm Description

The headland turning cost function and searching method for all possible dividing lines discussed above are important for coverage path planning. To design the optimal coverage path planning algorithm, a divide-and-conquer strategy was adopted. Specifically, for a given field f, the algorithm first searched for the optimal path direction d without any decomposition. The cost of this coverage was recorded as C. Then, instead of covering f as a whole, the algorithm tried all possible ways of decomposing f into two sub-regions. For each trial decomposition, the coverage cost was then calculated for the two sub-regions by recursively applying the algorithm to each of them. The sum of the two costs was recorded for the decomposition. This decomposition process was carried out in a recursive fashion so that all possible solutions were exhaustively investigated. If a summed cost of any decomposition was lower than the original cost C, then the decomposition with the lowest summed cost was returned. Otherwise, if no decomposition could provide a lower summed cost than the cost of covering the entire field as a whole, then the original results of d and C were returned as the output.

The optimal path planning (OPP) algorithm is outlined as follows:

Algorithm: OPP(f, w, r, W_h)

Input: f (planar subdivision of the field with boundary length and direction information), w (operation width), r (vehicle's minimum turning radius), W_h (headland width).

Output: A list of planar subdivisions representing the sub-regions, a coverage path direction for each region, and the total coverage cost.

Step 1: Find the optimal covering path direction and determine the most suitable headland turning type at each edge for the whole field f based on the turning cost function, where d is the path direction, and C is the cost of covering f with a boustrophedon path along direction d.

Step 2: Search for a collection of all possible ways of decomposing f into two regions.

Step 3: For each trial decomposition, say f_1 and f_2 are the two regions. Apply the OPP algorithm recursively to f_1 and f_2 with returned coverage costs of C_1 and C_2, respectively. If $C_1 + C_2 < C$, then this decomposition case is recorded.

Step 4: If there is no more valid decomposition, then return the results of step 1, or else return the case having the minimum $C_1 + C_2$.

End of algorithm.

Running Time Reduction

In addition to step 3 of the OPP algorithm described above, the time spent on searching for the decompositions dominated the required computational time for the algorithm. For a field with totally n edges, the time spent on the depth-first search was $T_d = O(n^3)$. In step 3, the OPP algorithm was called recursively on the two sub-regions, which assumably had a total of n_1 and n_2 edges. In addition, there were two restrictions: $n_1 + n_2 \leq n + 2m + 2$, where m is the number of obstacles in the original field, and $n \geq 3(m + 1)$ since there were at least three edges for each polygon. The total running time of the OPP algorithm (T_{opp}) was computed as:

$$T_{opp} = O[n^3 \log(n)] \tag{21}$$

Modifications to the optimization algorithm were made to reduce the computational time. First, when constructing the undirected graph for searching for the dividing lines, instead of drawing rays through each vertex to all directions, only the rays leading to new edges belonging to one of the following three categories were drawn: diagonals, line segments through the vertex and parallel to an edge, and line segments through the vertex and vertical to an edge. Adopting other dividing lines outside of these three categories would mostly incur more angled turns and thus increase the total turning cost. This improvement not only reduced the computational time but also eliminated the errors caused by using a big step size when drawing the rays.

The existence of obstacles significantly increased the running time. Smaller obstacles were unlikely to influence the decomposition scheme and the general direction of paths. It was also unlikely for the optimal dividing lines to go through any vertex of small obstacles. Therefore, internal obstacles with smaller areas were filtered out. The obstacles in this group would not be considered in the algorithm when searching for the dividing lines. While none of these improvements could change the form of asymptotic complexity given in equation 21, they could substantially reduce the expected running time.

Performance Evaluation

The OPP algorithm was first implemented in Java J2SE 5.0 (Sun Microsystems, Santa Clara, Cal.) and later transferred to Visual C++ 2005 (Microsoft Corp., Redmond, Wash.). The programs were tested on a computer with a 3.20 GHz Pentium 4 CPU and 1.50 GB of RAM. The pro–

grams were used to find the optimal decomposition and straight parallel coverage path directions for planar fields with various shapes. Some of the outputs were compared with both former researchers' results and farmers' actual driving patterns. For most of the tests, it was assumed by default that the equipment turning radius was 4.57 m, the swath width was 12.19 m, and the headland width was 24.38 m (exactly twice the swath width). Other settings were also assumed and adopted, which are specified in this article. These settings can easily be changed when real data are available.

RESULTS

For all tested fields with no more than 20 vertices and five interior obstacles, the optimal solutions were found by the OPP software within 60 s. Unless specified, it was assumed that the default settings described in the Performance Evaluation section above were adopted for the equipment turning radius, the headland width, and the swath width. According to the turning type decision tree (fig. 9), under this default assumption, "flat" turns should be adopted in most of the cases. In the following displayed examples, the selected turning types are not specified unless any turning types other than "flat" turns were adopted.

In figure 12, for the L-shape field, the best solution returned by the algorithm was to decompose it into two rectangular shapes with coverage path directions along the longer edges.

Hunt (2001) pointed out that because of the higher costs of angled turns, when covering a right-angled triangle field, it is better for the coverage pattern to be parallel to a perpen-

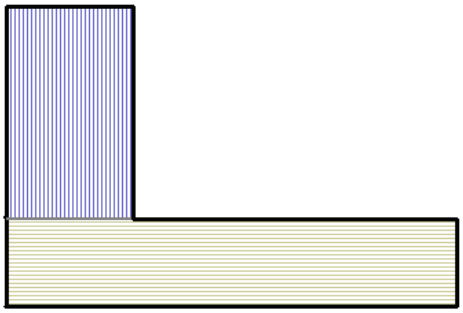

Figure 12. Field decomposition and path planning for an L-shape field.

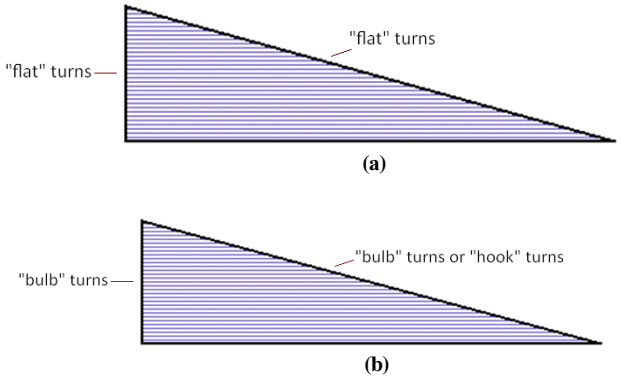

Figure 13. Path planning for a right-angled triangular field: (a) result when the assumptions of the equipment turning radius (4.57 m), headland width (24.38 m), and swath width (12.19 m) were adopted, and (b) result when the swath width was changed to 6.10 m.

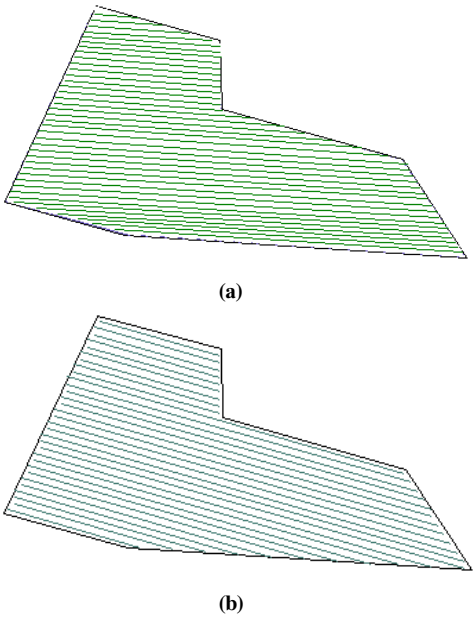

Figure 14. Comparison of OPP with conventional approach: (a) conventional approach of covering along the longest edge, and (b) OPP output.

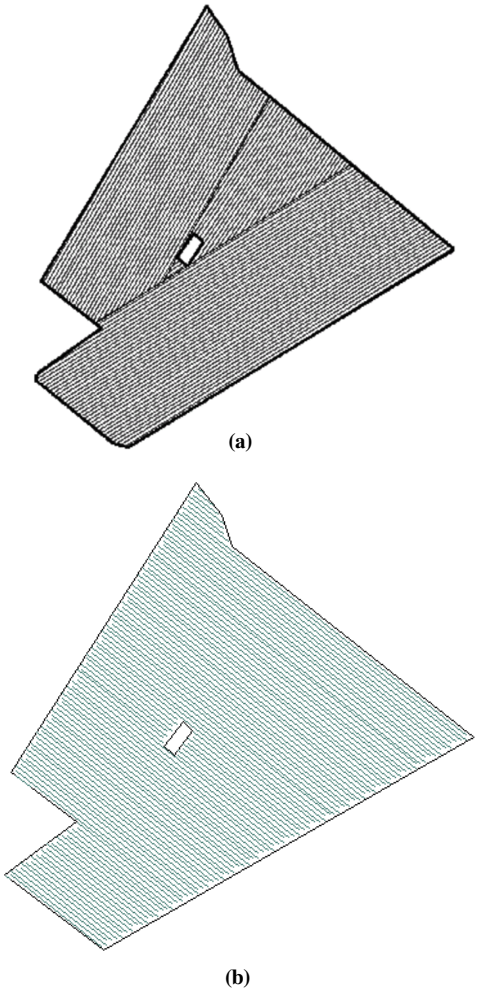

Figure 15. Comparison of OPP with other's approach: (a) approach of Oksanen and Visala (2007), and (b) OPP output.

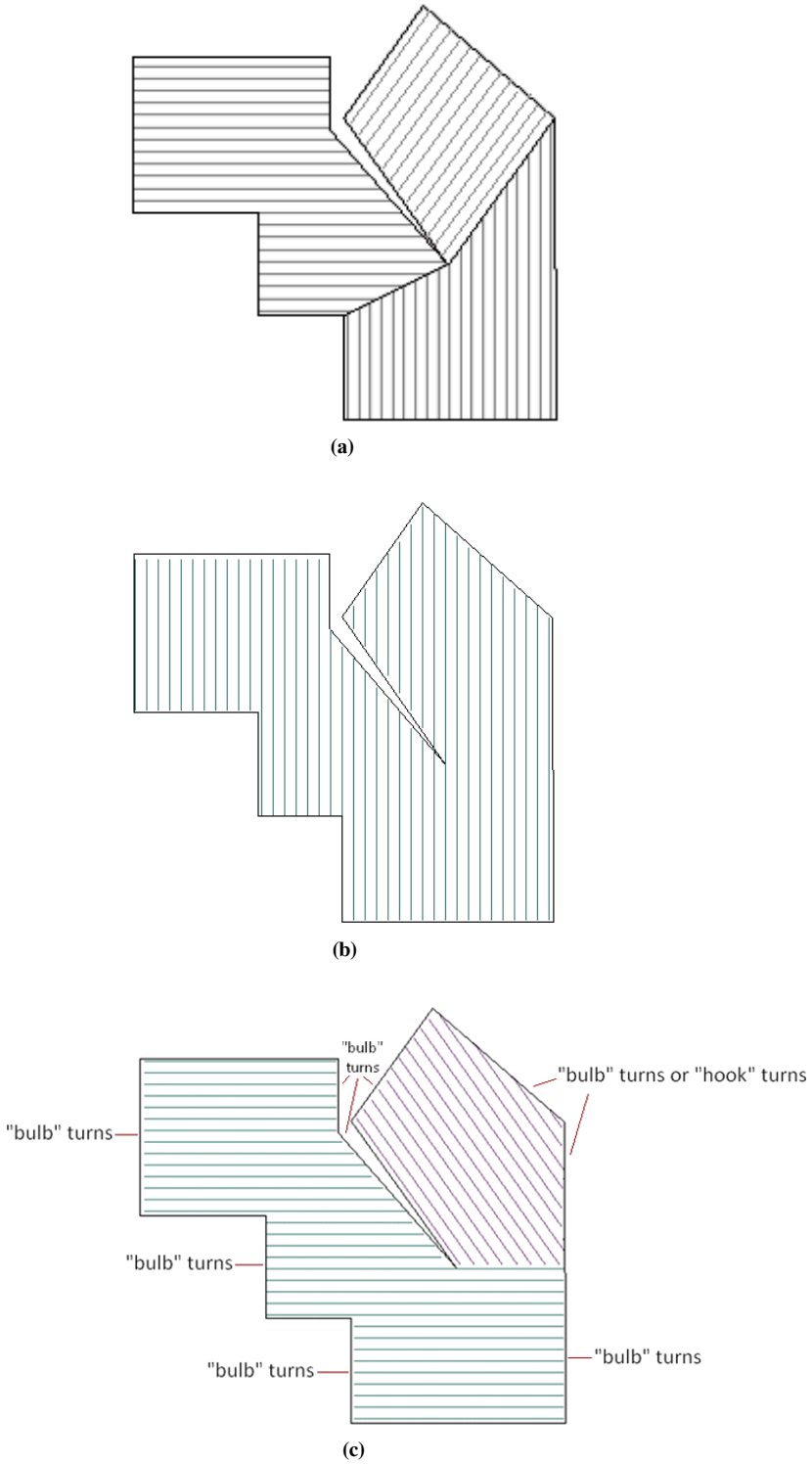

Figure 16. Comparison of OPP with others' approach: (a) approach of Fabret et al. (2001); (b) OPP output when the assumptions of the equipment turning radius (4.57 m), headland width (24.38 m), and swath width (12.19 m) were adopted (all turns were "flat" type in this result); and (c) OPP output when the swath width was changed to 6.10 m.

dicular side rather than to the angled side. This was confirmed by the OPP's results, shown in figure 13. Figure 13a shows the result when the default assumptions of the equipment turning radius, headland width, and swath width were adopted. All turns were of the "flat" type in this result. Figure 13b shows the result when the swath width was changed to 6.10 m (eight rows of corn plants). "Bulb" turns (or sometimes "hook turns") were adopted in this result because of the limited turning space.

Farmers tend to choose the longest edge direction as the coverage path direction (fig. 14a). However, sometimes there exist better solutions than traveling along the longest edge direction. In the following example (fig. 14b), the OPP made good use of the parallel relationship among three edges. Ac-

cording to the cost function described before, when compared with the solution in figure 14a, the solution in figure 14b saved 5% on the number of turns and 6% on the cost on the edges.

The results from the OPP algorithm were compared with the solutions generated by previous researchers. Figure 15a is an example given by Oksanen and Visala (2007), who adopted trapezoidal decomposition for path planning. There were lots of angled turns in their original plan. The solution generated by the OPP algorithm (fig. 15b) produced 4% greater number of turns, but the cost of the angled turns was reduced, resulting in a 15% reduction of turning cost on the edges.

Figure 16a is an example given by Fabret et al. (2001), who chose a "steering edge" to guide the motion direction, which was mostly the longer side of the field. Figure 16b shows the result of the OPP when the default assumptions of the equipment turning radius, headland width, and swath width were adopted. All turns were the "flat" type in this result. According to the cost function described before, the result in figure 16b saved 16% on the number of turns and 12% on the turning cost on the edges. Figure 16c shows the result when the swath width was changed to 6.10 m (eight rows of corn plants). Instead of being limited by using only diagonals as separation boundaries, the OPP found a better dividing line that started at one vertex and was parallel to the bottom edge. "Bulb" turns (or sometimes "hook" turns) were adopted in this result because of the limited turning space. The result in figure 16c saved 9% on the number of turns and 14% on the turning cost on the edges compared with Fabret's result in figure 16a.

The example given by Fabret et al. (2001) was studied further by adding two obstacles to the field. The result is shown in figure 17. If the former cover pattern in figure 16c was not changed, the result would look as shown in figure 17a. The OPP responded to the addition of the obstacles and obtained a new solution (fig. 17b) with no decomposition. Since the new obstacles brought some vertical edges into the field, it was reasonable to cover the field with vertical paths. According to the cost function described before, compared with the solution in figure 17a, the OPP saved 4% on the number of turns and 4% on the cost on the edges.

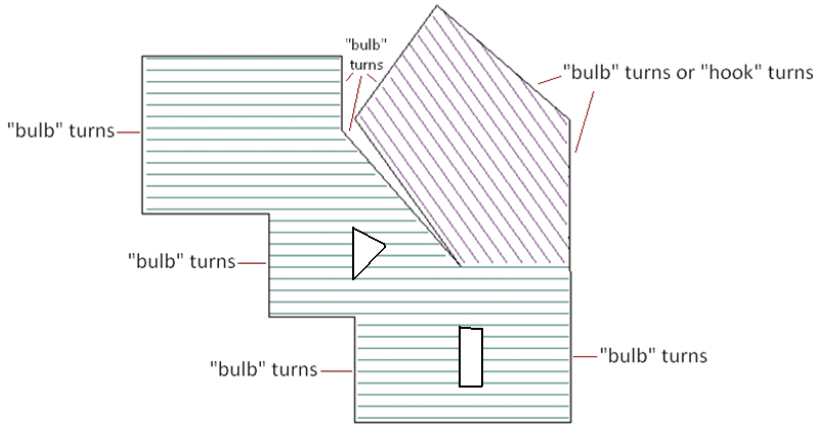

Figure 17. Adding two obstacles to the example field of Fabret et al. (2001): (a) unchanged approach of figure 16c, and (b) new OPP output.

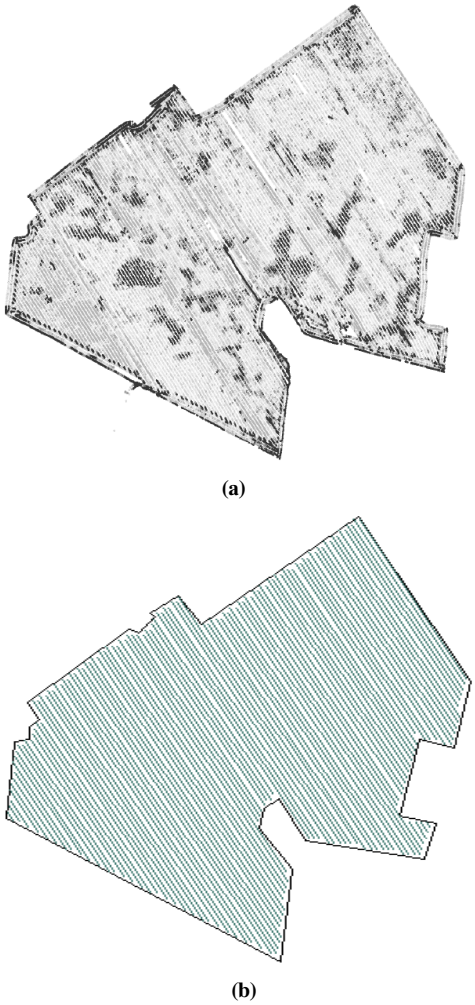

Figure 18. Comparison of OPP with farmer's approach: (a) harvesting operation trajectory on the yield map of farm field 1 in Ohio, and (b) OPP output.

Figure 19. Comparison of OPP with farmer's approach: (a) harvesting operation trajectory on the yield map of farm field 2 in Ohio, and (b) OPP output.

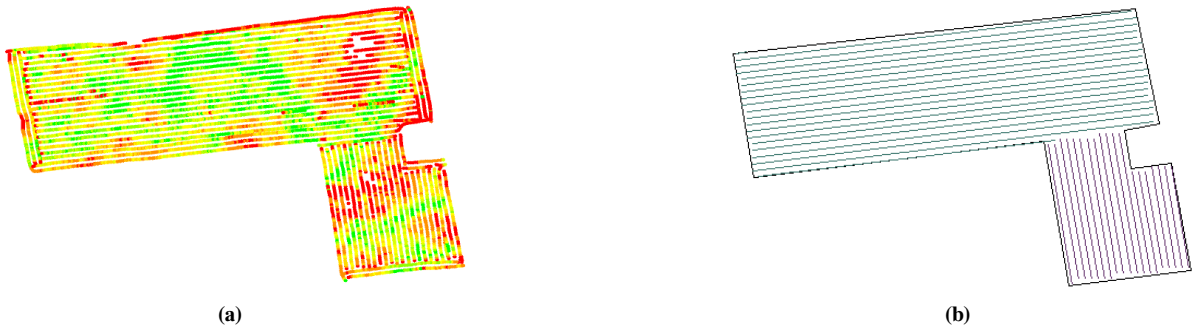

Figure 20. Comparison of OPP with another approach: (a) harvesting operation trajectory on the yield map of farm field 3 in Ohio, and (b) OPP output.

Figure 18 shows an example in which the OPP gave the same output as the farmer's choice. The paths were not along the longest edge. Instead, the direction of another shorter edge was adopted to reduce angled turn costs.

Figure 19 shows an example in which the OPP gave a different solution from the farmer's. Compared with the farmer's solution, the OPP's solution had fewer turns but more angled turns. According to the cost function, the overall saving from the OPP on the number of turns was 9%, and the saving on the turning cost on the edges was 4%.

Figure 20 shows another practical example in which the OPP gave the same output as the farmer's choice. The field was divided into two sub-regions in both solutions. The comparison between the OPP's results and other solutions in the examples above are summarized in table 1.

Table 1. Comparison between OPP's results and other solutions.

Field	OPP's Saving on Number of Turns (%)	OPP's Saving on Turning Cost (%)
Designed field (fig. 14)	5	6
Oksanen's field (fig. 15)	-4	15
Fabret's field 1 (fig. 16)		
With default assumption	16	12
With adjusted assumption	9	14
Fabret's field 2 (fig. 17)	4	4
Ohio field 1 (fig. 18)	0	0
Ohio field 2 (fig. 19)	9	4
Ohio field 3 (fig. 20)	0	0

Conclusions and Discussions

The OPP algorithm was developed to find the optimal solution for decomposing a field into sub-regions and determining the coverage direction within each sub-region. The search mechanism of the algorithm was guided by a customized cost function that was concerned with the cost of different types of angled turns in the headland. The complexity of the algorithm was $O[n^3\log(n)]$ for a field with n edges in total. Field examples with complexity ranging from a simple convex shape to an irregular polygonal shape that had multiple obstacles within its interior were tested with the OPP algorithm. For all tested fields with no more than 20 vertices and five interior obstacles, the program found optimal coverage solutions within 60 s on a computer with a 3.20 GHz Pentium 4 CPU and 1.50 GB of RAM. The OPP's results were compared with the results of former researchers or farmers' actual driving patterns. The results showed that, in the most extreme cases, the OPP saved up to 16% in the number of turns and 15% in headland turning cost. There were no cases where the OPP produced worse solutions than the farmers' solutions. These results indicated that the OPP algorithm was effective in improving field equipment efficiency on planar fields by producing an optimal field decomposition and coverage path direction in each sub-region.

There are multiple ways that the OPP algorithm can further be improved. First, only sequential turns are currently considered for headland turns. In practice, skip turns can be used to save headland space. The planning of swaths sequences and skip numbers is needed when skip turns are involved. Second, the current algorithm does not provide the optimal positions for entering and exiting the field, nor does it provide the best solution for traveling between different sub-regions. Searching for the best sequence of covering different sub-regions is similar to a "traveling salesman problem" and remains as our future work. Third, investigations are needed to design the best path around the obstacles when internal non-passable obstacles exist. Headland planting both around the outside boundary and around internal obstacles needs to be planned, too. In the current solutions from the OPP algorithm, all paths are in the form of straight lines. For fields with curved boundaries, adopting curved paths may further improve the operational efficiency. In the U.S., a great proportion of farmland has rolling terrain, and path planning on 3D terrain has a great potential to further optimize field operations. For 3D path planning, in addition to the headland turning cost, soil erosion, speed control on slopes, and topography impacts on the paths need to be carefully analyzed. In addition, there are operational issues, such as how to incorporate loading and unloading locations into the algorithm and how to coordinate multiple vehicles. Solving these problems remains as our future work.

References

Berg, M. D., M. V. Kreveld, M. Overmars, and O. Schwarzkopf. 2000. *Computational Geometry: Algorithms and Applications.* 2nd ed. Berlin, Germany: Springer-Verlag.

Choset, H., and P. Pignon. 1997. Coverage path planning: The boustrophedon cellular decomposition. In *Proc. Intl. Conf. on Field and Service Robotics*. Canberra, Australia.

Fabret, S., P. Soueres, M. Taix, and L. Cordessed. 2001. Farmwork path planning for field coverage with minimum overlapping. In *Proc. 8th Intl. IEEE Conf.* Piscataway, N.J.: IEEE.

Hunt, D. 2001. *Farm Power and Machinery Management.* Ames, Iowa: Iowa State Press.

Kise, M., N. Noguchi, K. Ishii, and H. Terao. 2002. Enhancement of turning accuracy by path planning for robot tractor. In *Proc. 2002 Automation Technology for Off-Road Equipment Conf.*, 398-404. St. Joseph, Mich.: ASAE.

Muller, D. E., and F. P. Preparata. 1978. Finding the intersection of two convex polyhedra. *Theoretical Computer Sci.* 7(2): 217-236.

Oksanen, T., and A. Visala. 2007. Path planning algorithms for agricultural machines. *Agric. Eng. Intl.: CIGR Ejournal* 4: manuscript ATOE 07 009.

Ryerson, A. E. F., and Q. Zhang. 2007. Vehicle path planning for complete field coverage using genetic algorithms. *Agric. Eng. Intl.: CIGR Ejournal* 4: manuscript ATOE 07 014.

Yang, S. X., and C. Luo. 2004. A neural network approach to complete coverage path planning. *IEEE Trans. Systems, Man, and Cybernetics: Part B. Cybernetics* 34(1): 718-725.